Programs and Algorithms of Numerical Mathematics 18
J. Chleboun, P. Kůs, P. Přikryl, K. Segeth, J. Šístek, T. Vejchodský (Eds.)
Institute of Mathematics CAS, Prague 2017

NUMERICAL STUDIES OF GROUNDWATER FLOW PROBLEMS WITH A SINGULARITY

Milan Hokr, Aleš Balvín

Technical University of Liberec
Studentska 2, Liberec, 46117, Czech Republic
milan.hokr@tul.cz, ales.balvin@tul.cz

Abstract: The paper studies mesh dependent numerical solution of groundwater problems with singularities, caused by boreholes represented as points, instead of a real radius. We show on examples, that the numerical solution of the borehole pumping problem with point source (singularity) can be related to the exact solution of a regular problem with adapted geometry of a finite borehole radius. The radius providing the fit is roughly proportional to the mesh step. Next we define a problem of fracture-rock coupling, with one part equivalent to the singular point source problem and the second part with a uniform flow. It is a regularized problem, but with the mesh dependence similar to the radial flow, in a certain range of steps. The behavior is explained by comparing the numerical solution with the analytical solution of a simplified problem. It also captures the effects of varying physical parameters.

Keywords: finite elements, mesh dependence, borehole, radial flow

MSC: 35A20, 65N30, 76S05, 86A05

1. Introduction

Although not mentioned among the main challenges in groundwater modelling, the issue of singularity, related to boreholes represented by a single point (in 2D) or line (in 3D), is not fully resolved, also because it is studied differently in theoretical work and in practical applications or simulation software.

The problem of point source in groundwater flow is shortly specified in 1.1. The singularity in the problem is a result of problem abstraction, convenient for handling the problem technically. The real case is that a borehole has a finite radius, but very small compared to the problem domain, which is inconvenient for meshing. On the other hand, a problem of a single borehole in homogeneous medium can be efficiently solved analytically. There are several either empirical or theoretical-based methods, introducing the analytical solution of the radial flow in the local scale to be coupled with a coarser mesh numerical solution – the analytical element

DOI: 10.21136/panm.2016.05

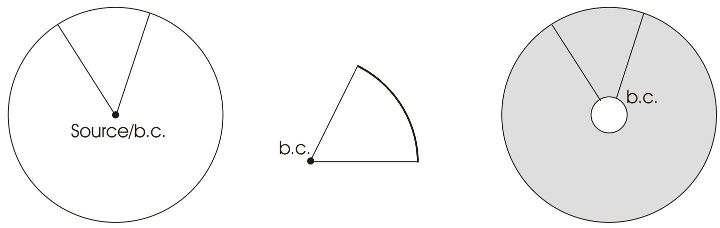

Figure 1: Left: radial flow around borehole in a singular form. Middle: configuration of boundary for numerical solution. Right: radial flow in a regular problem form.

method [2], Peaceman model in the field of reservoir engineering [6, 3], or the concept of extended finite element method (XFEM) with the enrichment functions based on the local analytical solution, e.g. [4].

The background is also different than studies aiming to approximate the singular problem solution and interpreting the numerical precision, e.g. [1] for the Dirac right-hand side with an a-priori set mesh refinement. Instead, we study the mesh dependence of the approximate solution in relation to a replacement problem, which gives a simpler understanding in the context of the finite borehole radius (alternatively to [3]). For such case, a sequence of fixed meshes is used, made by standard generators based on prescribed step at the boundary. This is subject of the first part of the paper and also a background for the second part, where we introduce a specific groundwater geometric configuration with analogous features but different interpretation of the mesh dependence.

1.1. Problem and singularity characterisation

The groundwater flow in its simplest form is a potential field, governed by linear Darcy's law and the mass balance equation,

$$v = K\nabla p\,, \qquad \nabla \cdot v = f\,, \tag{1}$$

where p is pressure head, v is flux density (velocity), K is hydraulic conductivity, and f are sources/sinks. Flux q meaning the integral of v is used in the solved problems.

In the borehole inflow configuration of Fig. 1, the singularity appears for the Dirac right-hand side, i.e. finite flux concentrated to a point as infinite spatial density, resulting to a generalised solution with infinite pressure at the point. Another formulation is with given finite pressure in the borehole, which can either be a boundary condition (formally, for the circular sector domain), or an additional constraint on the pressure solution together with related degree of freedom in the source/sink function f. The same is the asymptotic case of a finite borehole problem, solved analytically below.

For a real borehole, neither case is physically realistic, as the measured values of flux and pressure are always finite, and any kind of solution needs to introduce the borehole diameter as a parameter.

2. Borehole-driven radial flow problem

The example problem is a case of radial-symmetric flow into a borehole, which can be expressed either by a circle with the borehole in its center or by any sector of such circle (Fig. 1), with the radius r as one variable. The analytical solution is simply derived from 1D radial form of (1) by applying the separation of variables method. With pressure boundary conditions $p(r_1) = p_1$ and $p(r_2) = p_2$, the solution is

$$q(r) = 2\pi K \frac{p_2 - p_1}{\ln \frac{r_2}{r_1}}\,, \qquad \text{i.e.} \quad q(r) = \text{const} = q\,, \tag{2}$$

$$p(r) = p_1 + (p_2 - p_1)\,\frac{\ln \frac{r}{r_1}}{\ln \frac{r_2}{r_1}}\,, \tag{3}$$

considering the flux q over the full circumference. We see the singularity as the asymptotic behavior of the formulas for $r_1 \to 0$, i.e. $q \to 0$ for finite p_1 while $p_1 \to -\infty$ for a non-zero q. We study the first case in the following work, i.e. the dependence $q_{[r_1]}$, which is our notation for the parametric dependence on the problem geometry, to distinguish from the solution as a function of its space variable.

The study is based on comparison between the numerical solution of the singular problem with dependence on a mesh step h, and the analytical solution of the regular problem (2) with dependence on r_1. We use the circular sector geometry for the numerical problem (2D meshing). The boundary condition $p = p_1$ representing the borehole (singularity) is introduced to one node value of the standard finite element discretisation with piecewice linear base functions. The parameters used are $r_2 = 10$, $K = 1$, $p_1 = 0$ and $p_2 = 1$.

The comparison is made in two ways: the numerical $q_{[h]}$ dependence against analytical $q_{[r_1]}$ dependence for the choice $r_1 = h$ and an "inverse" problem of finding an effective borehole diameter r_1 to fit the numerical q value by the analytical one. We use more variants of mesh topology and, for each, a set of meshes of varying step h at the borehole boundary point is generated. So we can check other possible influences than the h value.

In the mesh set of type A, each refinement is generated independently, only based on the prescribed step h at the borehole and a different step along the outer boundary, resulting in either more uniform or more graded meshes. Three such sets of different domain angles $\varphi = 45°$, $60°$, and $90°$ are generated, denoted as A-45, A-60, and A-90. The set of type B, for $\varphi = 60°$ only, is constructed from the coarsest uniform mesh by sequential splitting of each triangular element uniformly, resulting in the same topology of all meshes in the set.

The results for a range of mesh steps are presented in Fig. 2. The parametric dependence of the flux is visually very similar between the analytical solution and

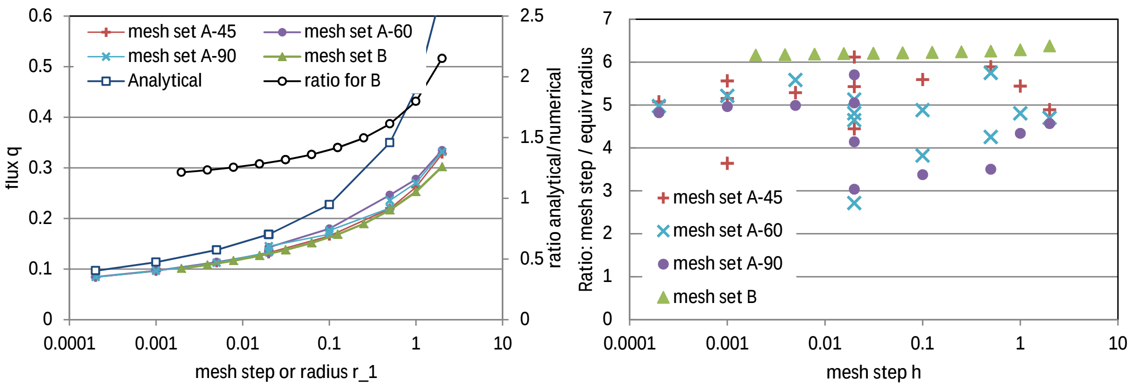

Figure 2: Relation of the numerical and analytical solution of radial flow for various mesh topologies: left is the resulting flux depending on either the mesh step or the borehole radius (scaled to equivalent of $\varphi = 60°$), right is the ratio of equivalent analytical solution radius (r_1) to a given numerical discretisation step.

the numerical solution (for $r_1 = h$), but the fluxes are not proportional, as seen from the evaluated ratio.

The effects of different meshes of the same h are often invisible for $q_{[h]}$, in general less then 10%, but they are detected in the inverse problem of effective r_1. The ratio of the given h and the fitted r_1, depending on h, is plot in Fig. 2 (right). The dependence can be evaluated as a constant, but with significant deviations related to different origin of the mesh. It leads to a hypothesis that the effective behaviour of the numerical solution with "point boundary" corresponds to the desired solution of the radial flow with particular radius, proportional to the mesh step. A precise relation could depend on the choice of numerical scheme and mesh topology.

3. Fracture-block coupling problem

3.1. Real-world motivation

The rock hydraulic conductivity K can change over many orders of magnitude and blocks of very different K are often parts of a single modelling problem. Within the low-permeable rocks, the water can be conducted along planes like fractures or tectonic faults; these are domains with orders of magnitude larger than K and small thickness. To get a measure of contribution to the total flux in a domain, the transmissivity is defined as a product of K and the thickness. If the fracture is represented as plane, the problem, in its vertical cross-section (2D), is a composition of a rectangle and a line (Fig. 3). It creates, at their contact, a singularity within the rectangle domain, similar to the borehole point source problem. Again, it is an effect of the model abstraction, while no sharp K changes or block edges would exist in the real rock.

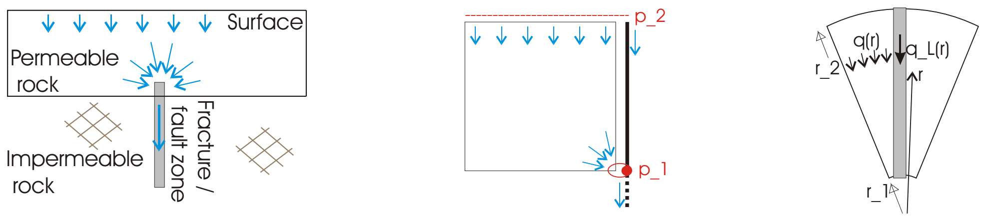

Figure 3: Left: real-world problem of fracture to permeable zone contact, which is in its part an analogue of the radial flow problem. Middle: model problem of fracture-porous block contact for the numerical study with the boundary conditions. Right: derived simpler analogue of coupled radial flow (circle) and uniform flow (line).

3.2. Problem configuration

The test problem to demonstrate numerical features is illustrated in Fig. 3 (middle). The configuration is an analogue of the problem in Decovalex-2015 benchmark [5], where the question of possible mesh dependence arised. Besides using reflection symmetry, there are two main differences against the real-world concept (Fig. 3 left):

One is in extending the fracture (line) domain along the whole rock (rectangle) domain in order to establish a communication between the domains which would not be possible for the mixed-hybrid finite elements through one node. Considering the fracture transmissivity is not significantly larger than the rock block transmissivity (realistic assumption because of the large rock volume), the problem should not be affected much quantitatively.

The second adaptation excludes the part of the line not in contact with the rectangle. The total flux is controlled by a "serial connection" of the line along the rectangle and the line below the rectangle. The latter is controlled by a linear relation of pressure gradient and flux, so the difficulty related to the singularity is present only in the rectangle part, which we concentrate on.

The domain dimensions are 50×50, as well as $r_2 = 50$ in the problem of Section 3.3 for comparison. The boundary pressure values are $p_1 = 0$ and $p_2 = 1$, and the coefficients are listed in Section 3.4.

3.3. Simplified analytical solution

To get an analytical solution for comparison, the problem needs to be significantly simplified (Fig. 3 right): a circular sector between two radii, r_1 inner and r_2 outer, and a line with coordinates between the same r_1 and r_2. We assume radial symmetry and ideal contact between the domains, i.e. a common value of pressure $p(r)$ for both the radial flow and the uniform flow. There are two variables for the flux, $q(r)$ in the circular domain and $q_L(r)$ in the line domain. For simplicity, we consider the unit thickness of the circular domain and the unit cross-section of the line domain, without loss of generality.

The system of equations for the choice of the circular sector angle φ is

$$q(r) + q_L(r) = \text{const} = Q, \tag{4}$$

$$q(r) = \varphi K\, r \,\frac{dp}{dr}, \tag{5}$$

$$q_L(r) = K_L \frac{dp}{dr}, \tag{6}$$

where K and K_L are hydraulic conductivities of the respective subdomains.

The analytical solution is a generalisation of the radial flow, with mostly technical differences. Substituting both q and q_L into the first (mass balance) equation, we get a form ready for separation of variables, p and r. Then two constants, the total flux Q and the integration constant, are evaluated from the two boundary conditions. The results are

$$Q = \varphi K \frac{p_2 - p_1}{\ln \frac{\varphi K r_2 + K_L}{\varphi K r_1 + K_L}}\,, \tag{7}$$

$$p(r) = p_1 + (p_2 - p_1)\,\frac{\ln \frac{\varphi K r + K_L}{\varphi K r_1 + K_L}}{\ln \frac{\varphi K r_2 + K_L}{\varphi K r_1 + K_L}}\,. \tag{8}$$

Additionally, we can derive $q_L(r)$ and $q(r)$. Then we evaluate the asymptotic problem behavior for $r_1 \to 0$. Obviously, the term K_L regularizes the solution, so that $Q_{[r_1]}$ converges to a finite value composed, at the boundary, of finite $q_{L[0]}(0)$ and zero $q_{[0]}(0)$.

3.4. Parameter sensitivity

The asymptotic behavior for $r_1 \to 0$ is strongly related to the magnitude of φK versus K_L, which is demonstrated in Fig. 4 for $K = 10^{-8}$ and two choices $K_L = 10^{-7}$ and $K_L = 10^{-10}$. For dominating conductivity of the circular domain (Fig. 4 left), the certain range of r_1 dependence is similar to the singularity case of the radial flow alone, requiring substantially small r_1 to exhibit the convergence through the contribution of the line domain. For small r_1, most of water comes through the line domain at the r_1 boundary and the flux $q_{[r_1]}(r_1)$ decreases much more quickly with r_1 than would for the pure radial flow problem. Contrary, for dominating conductivity of the line domain (Fig. 4 right), the q contribution quickly vanishes with decreasing r_1 and the changes of $Q_{[r_1]}$ are relatively smaller.

3.5. Numerical tests

We compare the dependence of the analytical solution on r_1 (total flux $Q_{[r_1]}$) with the dependence of the numerical solution (flux through the Dirichlet boundary bottom right corner) on mesh step h in Fig. 5. We note that, contrary to the previous case of radial flow, the solution used for the comparison is for a significantly simplified problem – in particular, not capturing that the 2D domain is not exactly radially symmetric and there is not necessarily an equilibrium between the domains. Two

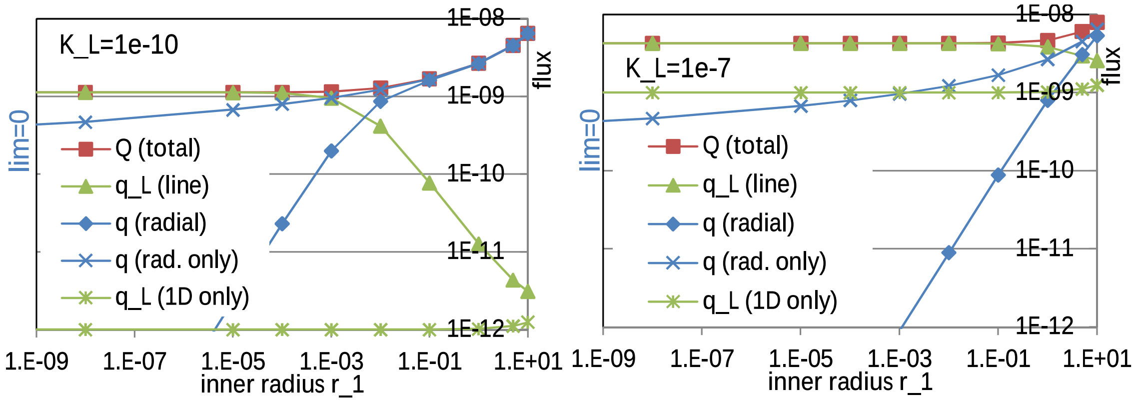

Figure 4: Analytical solution of the coupled circle-line flow problem showing convergence with decreasing inner radius, different for either dominant circle (left) or dominant line (right). The "radial only" and "line only" cases are solutions on each of the subdomains uncoupled, with the same boundary conditions.

different finite-element versions are used – the standard linear FEM with shared degrees of freedom of the rectangle side and the line and the mixed-hybrid (MH-FEM), with separate degrees of freedom.

There is a lot of common in the mesh-dependence with the radius-dependence, but the quantitative relation is not so clear as for the radial flow in Section 2. The mesh dependence disappears for sufficiently small h, which suggests the convergence of the solution like in the simplified analytical problem for $r_1 \to 0$.

The physical parameter sensitivity is also well reproduced: there is a little mesh dependence for large K_L (even negligible for $K_L = 10^{-6}$, not shown), contrary to the significant mesh dependence for small K_L, disappearing for very small h. The mesh step size, necessary for $Q_{[h]}$ to get steady, is typically one order of magnitude larger then the radius, for which the analytical solution dependence on r_1 disappear, and this position is roughly proportional to K_L (Fig. 5).

On the other hand, the trends of $Q_{[h]}$ differ between the numerical schemes. The standard FEM solution Q decreases with mesh refinement similarly to the analytical $Q_{[r_1]}$ (total flux). The MH-FEM solution rises with the mesh refinement, similarly to the curve of the analytical $q_{L[r_1]}$ (line-only flux). It can be explained by a structure of the discrete unknowns: in the used implementation of the standard FEM, the boundary condition is prescribed to a shared node while in the MH-FEM, the b.c. is introduced to the line (see the red b.c. circle in Fig. 3 middle), which is then coupled to the rectangle, making the line domain more significant for the overall hydraulic resistance.

The flux at the mesh refinement limit lies between the analytical solution for $\varphi = \pi/3$ and $\varphi = \pi/2$. It means that only a part of the numerical problem domain (corresponds to $\varphi = \pi/2$) is effectively covered by the flow, as it is deviated from the radial symmetry (more for larger fracture contribution).

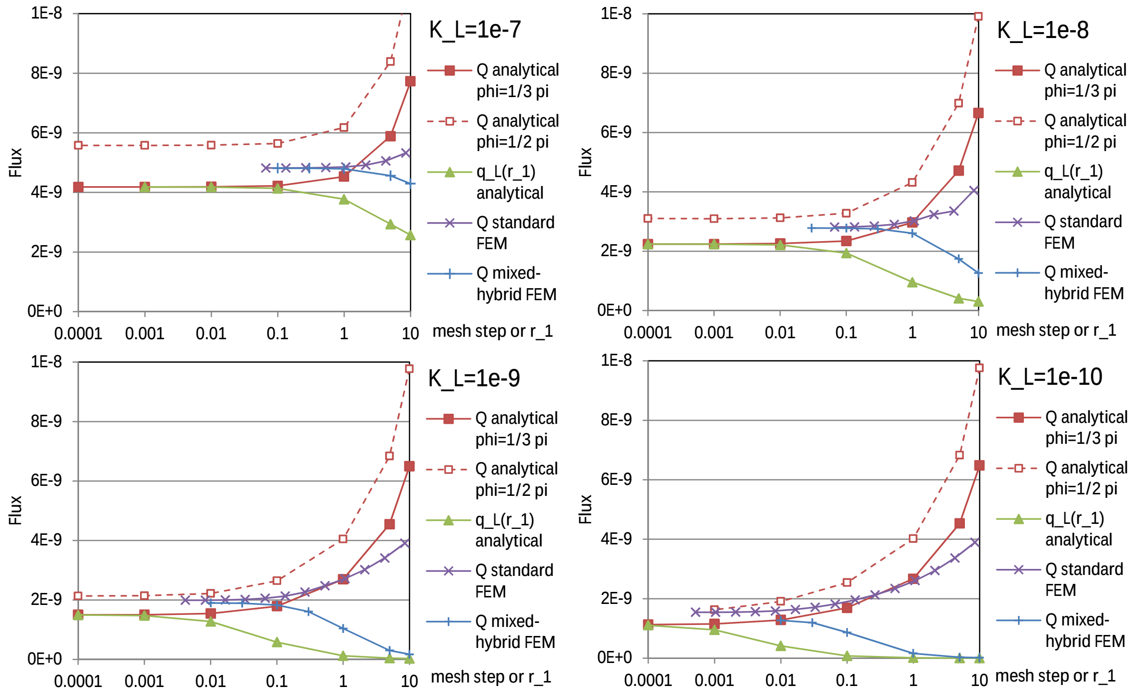

Figure 5: Mesh dependence of the block-fracture problem numerical solution compared to the radius dependence of the circle-line analytical solution (two choices of φ) for $K = 10^{-8}$ and a range of K_L, from fracture-dominant to block-dominant.

4. Conclusion

We have shown for the radial flow problem that the mesh dependence of the numerical solution, resulting from the singularity property of the point source/boundary, can have a physical meaning equivalent to the dependence of the real flow on the borehole radius. The mesh step providing the fit is roughly proportional to the borehole radius with a factor between 5 and 6 for meshes close to uniform while a larger deviation appears for more graded meshes. It could be a topic for further study to predict the relation theoretically from a numerical scheme. Such mesh choice can be useful as an alternative for adaptive mesh refinement based on error analysis. The error in flux is appropriate for groundwater data accuracy.

For the fracture-rock coupling problem, the extension of the fracture along the block regularizes the problem, although the mesh dependence is still present depending on the singularity component dominance. The mesh and the physical parameter dependence can be predicted by a relatively simple analytically solvable problem, in particular the position of visual convergence. Also, we have shown how the solution is sensitive on the position of the discrete unknowns.

Acknowledgements

This work was realised with the institutional support of the Faculty of Mechatronics, Informatics, and Interdisciplinary Studies, TU Liberec, and supported by the Radioactive Waste Repository Authority (SÚRAO), contract code SO2013/077.

References

[1] Apel, T., Benedix, O., Sirch, D., and Vexler, B.: A priori mesh grading for an elliptic problem with Dirac right-hand side. SIAM J. Numer. Anal. **49(3)** (2011), 992–1005.

[2] Bakker, M. and Strack, O. D. L.: Analytic elements for multiaquifer flow. J. Hydrology **271(1–4)** (2003), 119–129.

[3] Ding, Y. and Jeannin, L.: A new methodology for singularity modelling in flow simulations in reservoir engineering. Comp. Geosci. **5** (2001), 93–119.

[4] Exner, P. and Březina, J.: Partition of unity methods for approximation of point water sources in porous media. Applied Math. Comp. **273** (2016), 21–32.

[5] Hokr, M., Shao, H., Gardner, W.P., et al.: Real-case benchmark for flow and tracer transport in the fractured rock. Environ. Earth Sci. **75** (2016), 1273.

[6] Peaceman, D.: Interpretation of well-block pressures in numerical reservoir simulation. SPE J. **18(3)** (1978), 183–194.